PHYSICAL REVIEW D VOLUME 36, NUMBER 7 1 OCTOBER 1987

Monopole-flux and proton-decay limits from the Soudan 1 detector

J. Bartelt,* H. Courant, K. Heller, T. Joyce, M. Marshak, E. Peterson, K. Ruddick, and M. Shupe
School of Physics, University of Minnesota, Minneapolis, Minnesota 55455

D. S. Ayres, J. W. Dawson, T. H. Fields, E. N. May, and L. E. Price
High Energy Physics Division, Argonne National Laboratory, Argonne, Illinois 60439
(Received 22 January 1986)

Final results are presented from the search for magnetic monopoles and nucleon decay in the Soudan 1 detector, a 31.4-metric-ton tracking calorimeter located underground at a depth of 590 m. A detailed description of the detector is given. The possible existence of monopole catalysis of nucleon decay has been systematically incorporated into the analysis. During a live time of 1.0 yr, no candidates for grand-unified magnetic monopoles were observed, leading to 90%-confidence-level flux limits near 10^{-13} cm^2 sec sr.

I. INTRODUCTION

The experimental program at the Soudan mine in northern Minnesota is one part of an international effort by the high-energy-physics community to search for nucleon decays of the type predicted by grand unified theories. Though these underground detectors are optimized for the observation of nucleon decay, they are, of necessity, sensitive to a number of other processes. To varying degrees, they detect cosmic-ray muons, high-energy neutrinos, and a host of muon-induced electromagnetic and hadronic processes. Some of these detectors would be sensitive to magnetic monopoles, though to date none have been observed in any underground detector.

At the Soudan research site a 31-ton tracking calorimeter, Soudan 1, has been in operation on the 23rd level of the mine since 1981. A very-fine-grained 1100-ton calorimeter, Soudan 2, is under construction. This paper describes an in-depth analysis of data from approximately one year of live time in the Soudan 1 detector, focusing on the search for magnetic monopoles and monopole-catalyzed nucleon decay. Some of these data have been published previously,[1] as have results on cosmic-ray muons.[2]

Ever since Dirac postulated magnetic monopoles to explain the quantization of electric charge,[3] searches have been made for them in bulk matter, at particle accelerators, and in cosmic rays, without success.[4] In recent years, interest has been rekindled from a theoretical standpoint by the demonstrations of 't Hooft and Polyakov that monopoles appear in any grand-unification scheme which contains an unbroken U(1) for electromagnetism.[5,6] Added impetus has come from experiment, with the possible detection of a monopole with a superconducting induction coil,[7] although this result is now much more doubtful since there have been no new candidate events in a much longer running time.[8,9]

Grand-unification monopoles would carry a multiple of the Dirac unit of magnetic charge ($137e/2$), and would be extremely massive, about 10^{16} or 10^{17} GeV/c^2. Monopoles in Kaluza-Klein theories may be even more massive.[10] Hence even at relatively low velocities they would have enormous kinetic energies, and would be able to penetrate to a significant depth underground.

It should be noted that the number density initially predicted by some theoretical models was very high, much higher than experimental limits.[11,12] This contradiction has motivated modifications of the theories to reduce the number of primordial monopoles.[13,14] Some theories involve a period of exponential expansion of the Universe (inflation),[15,16] in which the initial, topological monopole density is approximately one per horizon; this would be unmeasurably small. Most of these models, however, allow enough later thermal production of monopoles to produce an experimentally interesting abundance.[17,18]

Independent of cosmological arguments, Turner, Parker, and Bogdan[19] have pointed out that astrophysical observations place upper limits on the possible flux of monopoles in our Galaxy (the "Parker" bound) which depend on the mass and velocity of the monopoles. These are based on the known strength of the galactic magnetic field (a few microgauss), and the fact that its regeneration time is not less than about 30×10^6 yr. Since the galactic B field would lose energy to magnetic monopoles by accelerating them, the amount of energy per unit time going into monopole acceleration cannot exceed the power going into regenerating the B field. These considerations set limits of 10^{-10} monopoles/cm^{2}sec sr (for $v=c$ and mass 10^{16} GeV/c^2), and 7×10^{-13} (for $v=10^{-3}c$ and mass 6×10^{19} GeV/c^2, the Kaluza-Klein value), for example. The most likely limiting value is about 10^{-15} monopoles/cm^{2}sec sr, for masses of 10^{16} GeV/c^2 and $v=10^{-3}c$, about one order of magnitude lower than experimental limits. It is possible, of course, that the local density and flux are higher; but there is no *a priori* reason to predict this. Very large detectors would be needed to be sensitive to a flux as small as the most likely value of the Parker limit. The limits on the known mass density of the Universe also can be used to set limits on the flux of monopoles.[20]

In any case, the unambiguous detection of a heavy monopole would not only be an important discovery in its own right, but would also lend strong support to grand unification.

The detection of a magnetic monopole with an ionization detector is critically dependent on the velocity of the monopole. The monopole velocity distribution is, however, unknown. Monopoles could be accelerated to a few percent of the speed of light by galactic magnetic fields,[19,20] but if this process is randomized by the chaotic nature of the fields, the characteristic velocity might only be $10^{-3}c$, that of the solar system through the Galaxy. If the monopole flux is enhanced by a mechanism which traps them in the vicinity of the Sun, the relevant velocity would be that of the Earth in its orbit ($10^{-4}c$) or the Earth's escape velocity ($3\times10^{-5}c$). While monopoles with a velocity of more than $10^{-2}c$ should ionize very heavily (more than 40 times minimum[21]), the ionization drops off very rapidly near a cutoff velocity. Ahlen, Liss, and Tarle[22] have calculated this to be about $2\times10^{-3}c$ in argon, the medium relevant to our experiment. Hence, below this velocity, monopoles would probably not be directly detectable in the calorimeter.

In addition to these properties, several theorists[23,24] have suggested that grand-unification monopoles should be able to catalyze nucleon decay with substantial (strong-interaction) cross sections. If this process occurs, the decay products of the nucleon will be relativistic, and detectable in an ionization calorimeter. Thus the process of monopole catalysis of nucleon decay would open a detection window below the velocity where direct observation of a monopole is possible.

We have searched, using the Soudan 1 detector, for four types of events that might be produced by monopoles: (1) particles which produce extremely large ionization (as monopoles with velocities in the range of $0.01c$ up to c would); (2) slowly moving particles ($0.002c$ to $0.01c$) which ionize and are able to penetrate the 590-m rock overburden; (3) single contained nucleon decays, as might be produced by nonionizing monopoles with small catalysis cross sections; and (4) multiple nucleon decays separated in time or nucleon decay(s) along a slow track (as might be produced by a slow-moving, catalyzing monopole). Preliminary data from some of these searches have been previously reported.

II. THE SOUDAN 1 DETECTOR AND ITS CALIBRATION

A. The calorimeter

The detector was constructed on the 23rd level of the Soudan iron mine, in northeastern Minnesota. The mine follows a roughly planar ore body at a 12° angle to the vertical. The surrounding rock is mostly Ely greenstone, with some jasper inclusions. The iron ore of the Soudan mine is an extremely high grade, nonmagnetic hematite. The average density of the greenstone and jasper is between 2.8 and 2.9 g/cm^3 from direct measurements of samples. The iron ore has a density of about 5.5 g/cm^3. A careful fit to the angular variations in the muon flux determined the overall average density to be 2.93 ± 0.05 g/cm^3. It should also be noted that the rock has an average value of (Z^2/A) of 6, somewhat higher than standard rock.

The detector, at a depth of 590 m [1800 m water equivalent (mwe)], is about 5 m east of the main access shaft (No. 8, the "Montana shaft"). The experimental area is about 20 m long, cut into a pocket of jasper. The width varies from 3 to 5 m, and the height is about 2.5 m.

The calorimeter consists of 432 modules or slabs, each containing eight proportional tubes embedded in heavy concrete (see Fig. 1). The steel tubes are 28 mm in diameter (with 0.8-mm-thick walls), 2.9 m long, and are filled with a standard welding-grade gas mixture of 91% argon and 9% carbon dioxide. The slabs are 4 cm thick, and the tubes are spaced 4 cm apart, horizontally, center to center. They are staggered vertically by 4.5 mm: the first tube in each layer is 4.5 mm lower than slab center, the second 4.5 mm higher, and so on. The average vertical distance from slab center to slab center (between adjacent layers) is 4.1 cm. Altogether, the detector is 2.0 m tall. The concrete has been loaded with taconite concentrate, an iron-rich, partially processed iron ore. Overall, the detector is 57% iron, 29% oxygen, 13% calcium, and 1.2% hydrogen, by mass. The density of the concrete is 2.49 g/cm^3; the average over the entire detector volume is 1.85 g/cm^3. This gives an average radiation length of 9.3 cm and a nuclear absorption length of 35 cm (these lengths were determined by measurements in a particle test beam, as described below). The total mass of the calorimeter is 31.4 metric tons, and it contains 1.9×10^{31} nucleons (1×10^{31} neutrons and 0.9×10^{31} protons, including 2×10^{29} free protons).

The slabs were stacked in 48 layers of nine slabs (72 tubes) each. The tubes in the first layer (and all the odd-numbered layers) are oriented roughly north-south; those in the even-numbered layers are orthogonal, lying roughly east-west. The odd-numbered layers give an X-Z view, the even-numbered a Y-Z view. From these two orthogonal two-dimensional views, a three-dimensional representation can be constructed for most events.

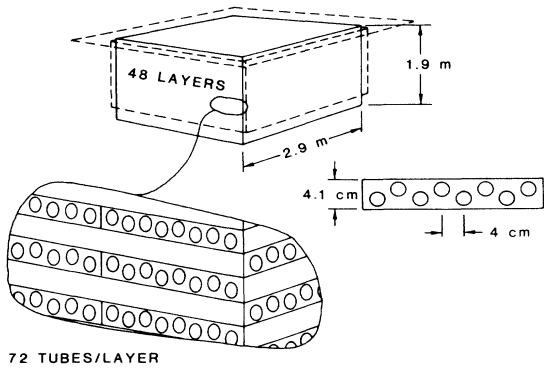

FIG. 1. A schematic view of the Soudan 1 detector. Dashed lines represent the position of the active shield.

The proportional gas is recirculated through a filtration system. It is fed in parallel to each of the 48 layers; it then flows serially through the tubes in each layer. After exiting the layers, it flows into a buffer tank, which sets the back pressure for the detector at 1 in. of water. Additional gas is automatically added to the buffer tank as needed to replace leakage. The gas flows from the tank, through the recirculating pump, then through silica gel (to remove water vapor) and activated charcoal (to remove organic molecules from the plastic tubing used on the detector), and finally back into the detector. The silica gel is held in metal cylinders, and is regenerated by heating and evacuating.

Each tube has a 50-μm, gold-plated tungsten central wire, which is maintained at 2200 V. The high voltage is supplied by a single computer-controlled supply to one end of all of the tubes in parallel. The other end of each wire is coupled through a 200-pF capacitor to a nearby amplifier via a twisted pair of wires, about 15 cm long. The total capacitance of the tube, decoupling capacitor and twisted pair is between 50 and 100 pF. Each channel uses one ECL (emitter-coupled logic) comparator chip (No. 10116) for amplification. The input resistance to the circuit is determined by an external resistor of 22 000 Ω in parallel with the chip's resistance of 50 000 Ω, for a total of 15 000 Ω and an RC time constant of 1 μsec. The signal goes through three amplification stages, each with a nominal gain factor of 12.

There are 16 channels on each amplifier board. To compensate for chip-to-chip variations, the threshold of each amplifier was determined by the voltage across the inputs to the third stage. This voltage was set to 400 mV for all 3456 channels, by adjusting a potentiometer which set the bias voltage for the first stage. Thus the input threshold for each channel is approximately 2.8 mV.

After amplification, the ECL signals are sent via ribbon cables to time-over-threshold (TOT) boards (see Fig. 2). The differential ECL pulses are converted to TTL (transistor-transistor logic) levels by line receivers on the TOT boards. From the line receivers, the signals are sent on two paths: one is for the trigger logic (see below) and the other is for the time-over-threshold circuit.

Since the pulses decay exponentially [with a decay constant (T) of 1.05 μsec, on the average], the time over threshold (t) is a logarithmic measure of the pulse height, and therefore also of the ionization deposited in the proportional tube (h). Thus,

$$h = Ke^{t/T} \tag{1}$$

or

$$t = T\ln(h/K)\ , \tag{2}$$

where K is the threshold ionization. The determination of K from the experimental data is described in the calibration section below. Sixteen-bit shift registers are used to hold the ionization information. If the pulse is over threshold, the input of the shift register is a logical 1; otherwise it is 0. The shift registers are clocked, initially, once every 185 nsec. A 50-nsec latch pulse is centered in the 185-nsec period; the data pulse must span the 50 nsec at least, in order to set the bit of the shift register. After a trigger, the clock continues for 14 counts. Then another shift register is clocked for 16 counts, once every 225 nsec. These 32 bins (16 "fast" and 16 "slow") preserve a 6.5-μsec history of the pulse, starting 370 nsec before the trigger.

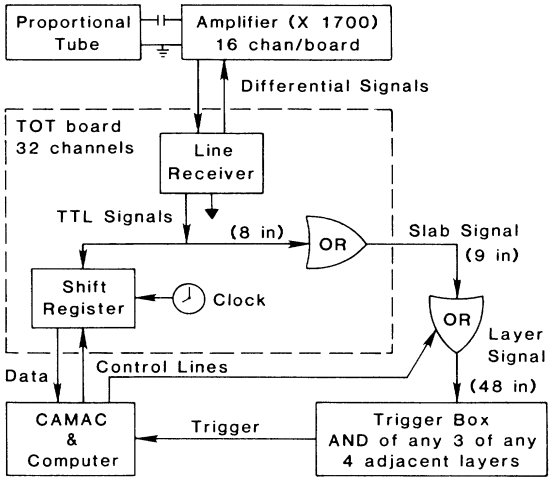

FIG. 2. A block diagram of the Soudan 1 electronics.

The trigger is formed via separate hardware. The pulses from the eight tubes in a slab are ORed together on the TOT boards. These slab signals are then fed to the first phase of the trigger circuitry. These circuits form an OR of the nine slabs in the layer; this OR is computer controlled, however, and any or all the slabs in a layer may be switched out of the OR. This is used to prevent a single noisy channel from driving the trigger rate too high; it does not affect the read-in of data from the TOT circuits. These 48-layer signals are fed to a trigger box; the trigger requirement is an AND of any three out any of four adjacent layers in coincidence, for at least 50 nsec. The trigger pulse is fed to a computer-controlled "scanner" circuitry, which controls the readout of the shift registers. Only those crates and boards (of time-over-threshold circuits) which contain nonzero data are read out. Additionally, an on-line software requirement that the event contain signals from at least five tubes was imposed. The buffer which initially holds the data is part of the computer memory; when it has a minimum of 512 bytes of data, and the computer is not otherwise busy, the buffer is written to a data file on disk.

Each event written contains pulse length and time information for each tube with a hit, data from the active shield (see below), the time and date of the event (from a crystal-controlled clock), and the event and run numbers.

B. The active shield

In order to more reliably detect charged particles entering or leaving the calorimeter, the Soudan 1 detector has been surrounded on the top and four sides by

scintillation counters which serve as an active shield (see Fig. 1). This aids in determining whether an event is truly "contained" in the calorimeter (as a nucleon decay or neutrino interaction inside the fiducial volume would be), or if it is caused by a particle or particles entering from outside. The shield can sometimes also detect a cosmic-ray muon which missed the calorimeter, but interacted in the nearby rock to produce a neutral particle which does enter and interact in the calorimeter. Such an event might otherwise appear to be contained. The timing information from the scintillator is also occasionally useful as a check on the velocity fit for monopole candidates.

The horizontal top counters are 1.2 m$\times$2.4 m$\times$1.25 cm thick and are composed of acrylic scintillator. They overlap 20–40 cm and overhang the calorimeter about 50–75 cm on the east and west sides, and about 40–60 cm on the north and south sides. On each of the four sides there are two (vertical) sets of four counters. Each side counter is a 0.9-m square, 2 cm thick, of pilot B scintillator. The top edge of the side counter array is approximately even with layer 48 (the top of the calorimeter.) This gives nearly completely coverage all around the detector, except for a 20-cm gap along the north edge of the west face, necessitated by cable trays. There are no counters underneath the detector.

Light from each of the top counters is conducted through an adiabatic light pipe into a 5-in.-diameter phototube. The side counters each have a 2-in. phototube abutting the middle of the scintillator; on the opposite face, there is a beveled notch to reflect light into the phototube.[25] The signals from the phototubes are sent to discriminators, and are then read in with the signals from the proportional tubes utilizing the same TOT electronics. The shield signal is not used in the trigger.

C. Efficiency, alignment, and calibration

Careful examination of mine surveys and topographical maps showed that the detector is 600($\pm$5) m underground, where this is measured to the top of the hill immediately above the detector. While the terrain drops by more than 50 m nearby, in no direction is the slant depth less than 590 m. These maps also indicated that the calorimeter's north-south axis is 5.7°$\pm$0.5° from true north. This was confirmed both by a gyroscopic compass carried from the surface to the 23rd level, and by the directional dependence of the muon flux, which is modulated both by the terrain and by the varying densities of rock.

Once the relative positions of the tubes and counters were established using straight-through cosmic-ray muons, other samples of straight muons could be used to measure the efficiency of the detector elements. Using straight-line tracks where the average deviation from the fit was 1 cm or less, the position of the track in each layer was calculated. If it passed within 5 mm of the center of a proportional tube, it was considered a predicted "hit." This 5-mm cut, which is less than half the tube's radius, allows for some margin of error in the tube's position and in the straight-line fit determined by the program. The event was then checked to see if that tube had been recorded. On average, the proportional tubes were 85–90% efficient, depending on running conditions. Similar methods showed that the shield counters 97–99% efficient, though in this case, the apparent inefficiency was due more to errors in track reconstruction than actual instrumental inefficiency. These numbers were used to quickly find any equipment failure, as indicated by a sudden drop in the measured efficiency.

Another measure of the calorimeter's overall efficiency (particularly useful on line) was a histogram of the ratio of the number of tubes in a track to the track length. When the detector was operating well, the median of this distribution varied from 0.150/cm to 0.158/cm, in good agreement with a Monte Carlo calculation based on 100% efficient proportional tubes which predicted 0.160/cm. The number of muons recorded per hour was also used to monitor the detector.

The ionization measurement provided by the pulse length information was calibrated by using a large sample of straight-through (nonshowering) muons. The first step was to eliminate channel-to-channel variations, by finding an average pulse length for each channel and dividing by the overall detector average pulse length. Then the exponential decay constant was determined by comparing the average pulse lengths of muons incident at various angles. Because of their longer path lengths in the tubes, muons that are more nearly horizontal should have longer pulses. Since the ionization deposited (h) is proportional to the particle's path length through a tube, the ionization in an x tube (for example) is proportional to the cosine of the y component of the zenith angle (θ_y). Thus,

$$h(\theta_y)=h(0)\cos(\theta_y)=Ke^{t/T} . \tag{3}$$

Thus the magnitude of the pulse length increase is equal to the decay constant (T) times the logarithm of the cosine of the y component of the zenith angle, or

$$t(\theta_y)=t(0)-T\ln[\cos(\theta_y)] . \tag{4}$$

From this we obtained a detector average of 1.05-μsec exponential decay time (in agreement with expectations from the approximately 1-μsec RC time constant), and an average pulse length for vertical-equivalent muons of 1.3 μsec. Since the average energy of a vertical muon in the detector is about 100 GeV (and higher for muons with nonzero zenith angles), the average ionization loss is well into the density effect plateau where the ionization has saturated and is independent of the incident particle's velocity at 1.58 times minimum.[26] Since

$$t=(1.05\ \mu\text{sec})\ln(h/K) , \tag{5}$$

we can determine the constant K from the known case of the muons; for $h=(1.58\times\text{minimum ionizing})$, and $t=1.3$ μsec, we find that $K=(0.458\times\text{minimum ionizing})$, on average. Thus we expect that a minimum-ionizing particle would produce pulses about 820 nsec long, or a little more than four bins. Even $\frac{1}{2}$-minimum-ionizing particles would be detectable, though their average pulse length would be only about 95 nsec; this is longer than the

latch pulse, and some tubes would have one bin pulses recorded.

In order to determine other properties of the detector, three small calorimeter modules, of the same construction as the experimental device, were placed in the High Energy Physics Text Beam at the Argonne National Laboratory Rapid Cycling Synchrotron. Protons, pions, muons and electrons of momenta from 150 to 400 MeV/c were used to measure radiation and interaction lengths, and to confirm the appearance of muon decays, the rise in ionization near the end of a stopping particle's track, and shower development. These data[27] were then used in a Monte Carlo program along with EGS3 (Ref. 28) shower simulations to model nucleon decays. Figures 3(a) and 3(b) show examples of the calibration data, the electron energy calibration and the muon range resolution, respectively.

III. DATA ANALYSIS

The raw data files were initially analyzed to select 12 types of events, including straight-through muons, nucleon-decay candidates, and monopole candidates. Our search for monopole candidates is, experimentally, a search for three distinct effects: the high ionization but substantial track length of a relativistic monopole, the slow velocity and substantial track length of a monopole traveling just above the velocity threshold for ionization, and/or the presence of single or multiple nucleon decays catalyzed by the monopole. Fours sets of criteria were used in selecting monopole candidates.

High-ionization candidates were required to have (1) between 8 and 50 hits in the fit, (2) at least 2 hits in each view, (3) the ratio of the hits in the fitted track to the total number of hits greater than 0.7, (4) the average deviation of the hit tubes from the fitted track less than 3 cm, and (5) the average normalized pulse length of the track greater than 3.7 μsec.

Low-velocity-fit candidates had to satisfy the requirements that (1) the χ^2 per degree of freedom be between 0 and 6 for the straight-line velocity fit, (2) the velocity of the track be more than four standard deviations below c, (3) the velocity be less than $0.01c$, and (4) the fit have more than 4 degrees of freedom.

The nucleon-decay candidates met the following criteria: (1) the shield counters were functioning well during the data run (at least 39 of the 40 counters were functioning properly, as shown by the number of hits in each); (2) the detector efficiency was good, as measured by the number of muons per hour detected (i.e., the number per hour did not deviate by more than 25% from the average); (3) the event was not flagged as having "bad data" (internally inconsistent format); (4) the event consisted of between 8 and 40 hit tubes (this corresponds to a total energy release of 0.5–2.5 GeV); (5) there were at least 2 hits in each view; (6) when a straight-line fitted track was extrapolated to the outside of the detector, no shield counter within 10 cm of the track was on; (7) either the top end of the event, or the bottom end of the event, or both, were at least 20 cm from the nearest face of the detector. These criteria

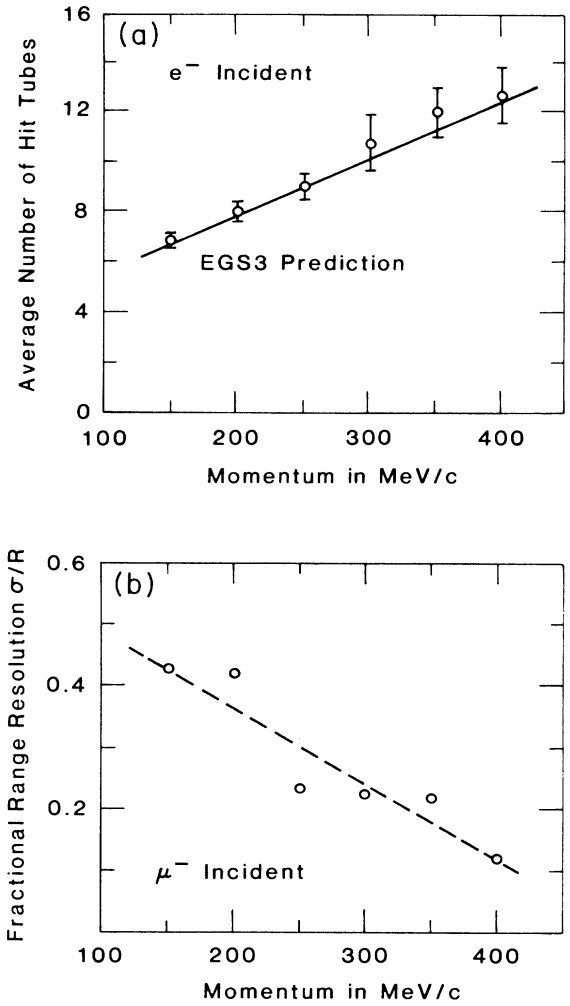

FIG. 3. (a) A comparison of electron energy-loss data from a test-beam exposure and Monte Carlo predictions, using the EGS3 simulation. (b) Range resolution of negative muons vs incident muon momentum from a subset of the test beam data. The best fit is shown as a dashed line, and was used to calibrate the Soudan 1 Monte Carlo program.

were optimized to find events contained within the calorimeter, and to eliminate events produced by cosmic-ray muons.

Nucleon-decay catalysis candidates were required to satisfy either the standard requirements for nucleon-decay events as described above (single-decay events) or, for multiple time-separated events, that (1) the total number of hit tubes be between 12 and 500 and (2) the number of late hits be between 7 and 500 ("late" means starting at least 550 nsec after the nominal trigger time).

The searches for candidates in these four data samples are discussed below. The possible presence of monopole catalysis of nucleon decay introduces various complications to this search procedure.

A. Acceptance

The most uncertain factor in calculating our acceptance for magnetic monopole events is the cross section

for nucleon-decay catalysis. We have parametrized the cross section as

$$\sigma = X\sigma_0(c/v) , \tag{6}$$

where X is an arbitrary factor presumably of order 0.001–1000.0, which scales σ_0, a typical strong-interaction cross section, 441 μb (the inverse of the square of the proton mass, in natural units). v is the magnitude of the relative velocity between the monopole and the nucleon. For free protons (i.e., hydrogen nuclei), this is just the monopole's velocity. For other nucleons, we have taken an average over the vector sum of the Fermi motion and the monopole's velocity. Because the average Fermi velocity is near $0.2c$, the catalysis probability is dominated by the 1.2% free hydrogen in the detector for velocities of $0.001c$ or less. Catalysis of nucleon decay in nuclei may be further suppressed (at these low velocities) by a distortion of the nucleon's wave function near the monopole by the long-range interaction of the electric and magnetic fields.[29] Conversely, the positive anomalous magnetic moment of the proton may provide an attractive potential between the proton and the monopole.[23,29] Thus the velocity dependence of the cross section at low velocities could be proportional to $(1/v)^2$ for protons. We have not taken explicit account of this enhancement, but it can be included in the arbitrary factor X. Because of the large uncertainties, we have made acceptance calculations for a range from 0.001 to 1000.0, and for $X=0$ (no catalysis).

We have also taken into account the possibility of a monopole catalyzing a nucleon decay in the rock wall, and the daughter particles of the decay entering and triggering the detector. This is particularly important with slow monopoles, which might not enter the detector during the 6.5 μsec the data is recorded, but would easily pass through the calorimeter during the resultant 1-sec dead time after the trigger. It is very unlikely that any such events, consisting solely of nucleon-decay fragments, would pass the scanning criteria. Because of this, our acceptance for monopoles is a complicated function of cross section and velocity. If the cross section is large, catalysis events in the detector become more probable, but so do events triggered solely by the daughters of rock catalysis events. The only practical way to determine this acceptance has been to use a Monte Carlo simulation.

This simulation propagated monopoles through 1 m of rock before they entered the calorimeter. If decays were catalyzed in the rock, and if the daughter particles had sufficient range and the proper orientation, they entered the calorimeter. (The rock was treated much the same as the calorimeter, except that it has slightly higher density, and less water, and therefore less hydrogen.) Particular attention was paid to the time of flight of the monopole from the rock to the calorimeter, and of the possible triggering of the readout by nucleon-decay fragments from the rock. The events generated were then processed by the sorting and selecting program, and the output files were scanned in the same way as the data.

(a)

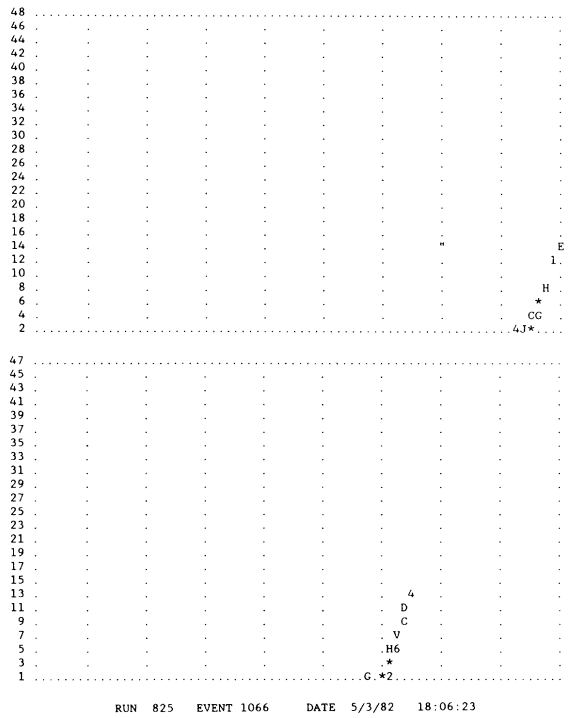

(b)

RUN 825 EVENT 1066 DATE 5/3/82 18:06:23
4 SHIELD HITS - # 2 8 29 31

LAYER	TUBE	FAST RAM	SLOW RAM
1	46	0111111111111111	1000000000000000
1	48	0111111111111111	1111111111111111
1	49	0001100000000000	0000000000000000
2	66	0111100000000000	0000000000000000
2	67	0011111111111111	1111100000000000
2	68	0111111111111111	1111111111111111
3	49	0111111111111111	1111111111111011
4	69	0011111111111111	1100000000000000
4	68	0111111111111000	0000000000000000
5	49	0011111111111111	1110000000000000
5	50	0111111000000000	0000000000000000
6	69	0111111111111111	1111111111111111
7	50	0111111111111111	1111111111111110
8	70	0111111111111111	1100000000000000
9	51	0011111111111100	0000000000000000
11	51	0011111111111110	0000000000000000
12	71	0000100000000000	0000000000000000
13	52	0001111000000000	0000000000000000
14	56	0101010001111100	1111111111111111
14	72	0111111111111110	0000000000000000
SHLD	2	0010001010000001	1000000000000000
SHLD	8	0010000110000000	0000000000000000
SHLD	12	0000000000000000	0000011000000000
SHLD	18	0000000000000000	0000000011000000
SHLD	29	0010000000000000	0000000000000000
SHLD	30	0000000000001000	0000000000000000
SHLD	31	0010000000000000	0000000000000000

FIG. 4. (a) Geometrical display of a high-ionization monopole candidate event. Each dot represents a tube position (in the interior, only every eighth tube is shown). The even layers provide an end view of the event, facing west, while the odd layers show the orthogonal view from the north. Letters and numbers ($A=10$, $B=11$, . . .) represent pulse lengths, in bins. Since some showering is evident, this is not a monopole. (b) Pulse profiles for the event in (a). The fast random-access-memory timing is 185 nsec/bin, the slow ram bins are 225 nsec. Tubes are numbered left to right in (a). Shield counters 1–8 are on the top of the detector, 9–40 comprise the sides. Counters 2, 8, 29, and 31 are in time with the event while counters, 12, 18, and 30 indicate random noise pulses.

B. The search for highly ionizing monopoles

To search for highly ionizing particles, we have set our ionization threshold at 16 times minimum ionizing, or about 10 times that of a typical muon. This corresponds to an average pulse length of 3.7 μsec, and eliminates nearly all nonshowering muons. Electromagnetic showers produced by muons do have a core of very high ionization; the requirement that no more than 30% of the tubes in the event be outside of the fit track helps to eliminate these. The distribution of average pulse lengths falls off very rapidly; we have, in effect, selected and examined the tail of this distribution. The selected events were found to have very short tracks with a few anomalously long pulses, or muons with narrow showers which pass our cuts. An example of the second type is shown in Figs. 4(a) and 4(b). Both the east-west (even) and north-south (odd) projections are shown, with numbers and letters in Fig. 4(a) indicating the number of time bins above threshold ($A=10$, $B=11$, etc.). Dots indicate unhit tube positions and other symbols indicate malfunctions. The time profiles of the individual pulses are shown in Fig. 4(b). We have found no events with consistently high ionization along a nonshowering track.

For our flux limit, we have conservatively estimated that the ionization produced by a monopole would be above our 16× minimum threshold only for velocities equal to or greater than $10^{-2}c$. (Ritson,[21] however, calculates ionization of this level for velocities above $0.005c$; and that at $0.01c$, the ionization would be 40 times minimum. This would correspond to pulses 4.7 μsec long.) If there is no nucleon-decay catalysis, our acceptance is a purely geometrical quantity. The geometric cross section of the detector, averaged over all angles, is 8.3 m^2. Taking into account the trigger and analysis efficiency and assuming an isotropic monopole flux, yields a total acceptance of 83 m^2sr. Together with our live time of 1.01 yr, this yields a flux limit (at 90% confidence) of 8.8×10^{-14} monopoles/cm^2sec sr, neglecting possible interference from the catalysis process. If the cross section for catalysis is large, however, events are lost from this category because the pulses produced by the nucleon-decay fragments reduce the average pulse length for the event below the threshold for computer identification. For cross sections of 44.1 mb ($X=100$) this effect reduces our sensitivity by a factor of 20 at $v=c$, the worst case. The events which are lost are characterized by large numbers of hit tubes, in patterns that resemble those from a series of hadron-nucleus collisions, or from muon electromagnetic showers. Both of these types of background events are numerous and the analysis procedure rejects them automatically.

C. The search for slow monopoles

To search for monopoles in the velocity range $0.002c-0.01c$, we fit velocities by using the starting times of the pulses in the various tubes. A straight-line fit to a track with constant velocity was required. The criteria for the velocity-fit events were optimized to eliminate muons, while retaining as large a fraction of the desired events as possible (guided by Monte Carlo studies). Our best possible time resolution is 185 nsec, but this is degraded by drift times which can be as large as 400 nsec. It is possible, for example, for a muon track to mimic that of a nonrelativistic particle because the drift times in the proportional tubes can vary from 0 to 2 bins (or more, in some cases), depending on how close the muon passes to the collection wire. We also find that electromagnetic showers often contain late hits. These, along with the late pulses from a muon decay, can contribute to an apparent nonrelativistic velocity. Thus we cannot reliably measure a velocity greater than $0.01c$, and we have set fairly stringent requirements on the fit to the velocity and straight line, to eliminate background events. We have assumed that monopoles in the velocity range of $0.002c-0.01c$ would not ionize sufficiently to meet our criteria for high-ionization events, but would produce enough ionization to be detected in the proportional tubes.[22]

Only one event has met these requirements (with an apparent velocity of $0.008c$), and we believe it to be a muon which has, by chance, simulated a nonrelativistic velocity well enough to pass our cuts. This belief is substantiated by the fact that its pulses are of normal length (indicating normal ionization), in contrast with our expectations of ionization several times greater than that of a muon; Ritson,[21] in fact, calculates the ionization at this velocity to be 30 times minimum (19 times as much as a muon), corresponding to pulses 4.4 μsec long (more than 23 bins of 185 nsec). The actual average pulse length for the event is 1.5 μsec. It is shown in Figs. 5(a) and 5(b), with the convention that the numbers and letters represent the time bin of the start of the pulse, rather than the pulse length.

If the cross section for catalysis becomes significant at these velocities, our acceptance for these events becomes smaller. The monopoles would be slow enough so that their tracks and/or the decays might contain late hits. This can degrade the fit (raising the χ^2, for instance), and events would then be lost from the velocity-fit category. Most of these would be found, however, by the catalysis search described below.

D. The search for single nucleon decays

During a live time[30] of 0.97 yr (during which about 1.02×10^6 single-muon events were recorded), 3400 events met the seven selection criteria described above for single, contained nucleon decays. These events were then scanned on video terminals by physicists. Of the 3400, more than 75% were rejected because they were caused by electronic noise or by radioactive decays within the detector, or because they passed the cuts due to misinterpretations by the simple straight-line fitting program. Another 20% were rejected for having shield counters registering near the fitted track, but not directly in its path. These events were primarily the result of muons producing showers in the surrounding rock, whose tail of soft particles reached the detector. Thus some low-energy particles (which did not penetrate the calorimeter) were detected by the shield counters, while

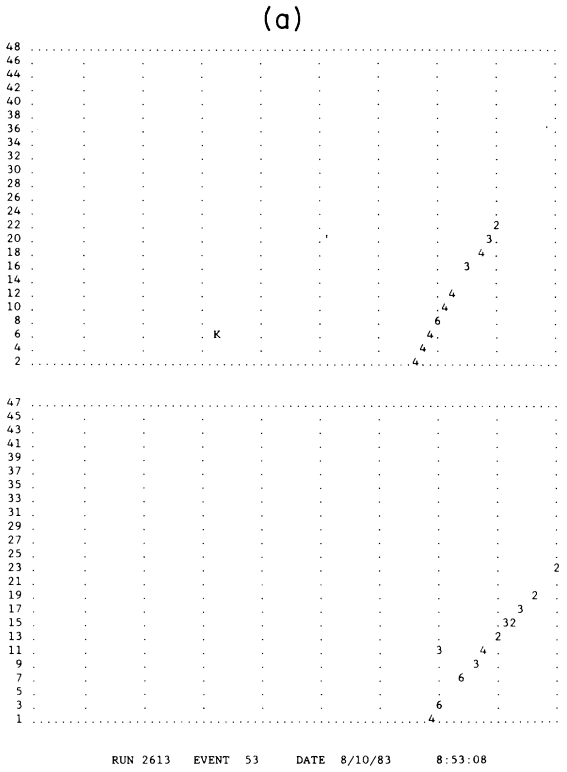

(b)

RUN 2613 EVENT 53 DATE 8/10/83 8:53:08

LAYER	TUBE	FAST RAM	SLOW RAM
1	55	0001110000000000	0000000000000000
2	53	0001111110000000	0000000000000000
3	56	0000011111000000	0000000000000000
4	54	0001111000000000	0000000000000000
6	26	0000000000000000	0001100000000000
6	55	0001111111000000	0000000000000000
7	59	0000011100000000	0000000000000000
8	56	0000011111100000	0000000000000000
9	61	0011111111000000	0000000000000000
10	57	0001111100000000	0000000000000000
11	62	0001111000000000	0000000000000000
11	56	0011111110000000	0000000000000000
12	58	0001111000000000	0000000000000000
13	64	0111111110000000	0000000000000000
15	66	0111111111111110	0000000000000000
15	65	0011111111111111	1111111111000000
16	60	0011111111111111	0000000000000000
17	67	0011111000000000	0000000000000000
18	62	0001111111000000	0000000000000000
19	69	0111111111111110	0000000000000000
20	63	0011111110000000	0000000000000000
20	41	0000000000000000	1000000000000000
22	64	0111111100000000	0000000000000000
23	72	0111111111111000	0000000000000000
SHLD	36	0011011100000000	0000000000000000

FIG. 5. (a) Display of an event that met the velocity selection criteria for a monopole candidate. Here numbers and letters represent the pulse start time bin relative to the trigger time. The pulse lengths, given in (b), are normal, indicating that this is not a monopole. (b) Pulse profiles for the event shown in (a). While the apparent velocity of the particle is 0.008c, the ionization is inconsistent with a monopole interpretation.

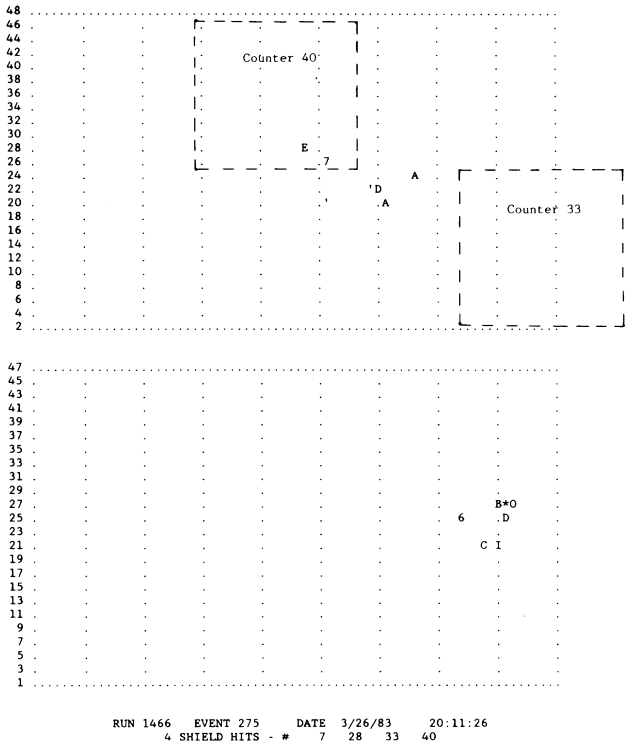

FIG. 6. A rejected candidate for nucleon decay. Four shield counters have signals in time with the event: counter 7 is on the top of the detector, directly above the active tubes. Counters 33 and 40 are indicated in the figure, and are on the face of the detector nearest the active tubes. Counter 28 is not near any hit tube. The counters indicate that the event was caused by particles entering the detector from the outside, and not by a contained nucleon decay.

other particles, or the muon itself, would enter the calorimeter nearby. An example of a rejected event of this class is shown in Fig. 6. Other events, almost 2%, were rejected because, though they did not shield counters on, they were topologically similar to the 20% just described, and were very near the face of the calorimeter. Since a small fraction of the cosmic-ray muons can penetrate the detector without producing a signal in the shield or first few layers of the detector, about 2% of the 3400 events, which were straight nearly vertical tracks, were rejected as being muons. Two events were then left, shown in Figs. 7 and 8. We consider neither event to be a good nucleon-decay candidate. Both events have a total apparent energy, based on the number of proportional tube hits as calibrated in the detector test beam run, of 650±200 MeV. From Monte Carlo studies the apparent mean energy expected for a decay event ranges from 820 to 940 MeV, depending on decay mode, with an uncertainty of 290 MeV. One possibility for these events is neutrino interactions in the detector. Since we expect that only 1.3 contained neutrino events would have been observed during our live time interval, and that only one-third of these would have had a structure similar to that of these events, this explanation is unlikely. A more probable hypotheses is

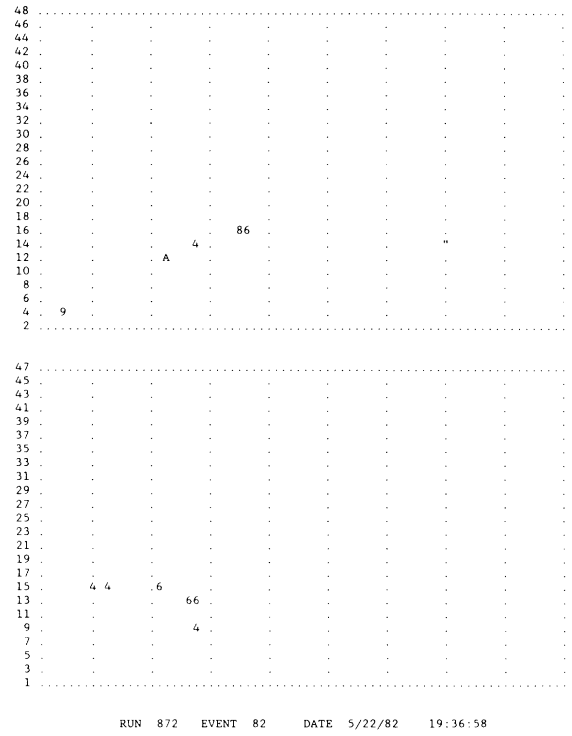

FIG. 7. The first contained event meeting the criteria for nucleon decay. See text for a discussion.

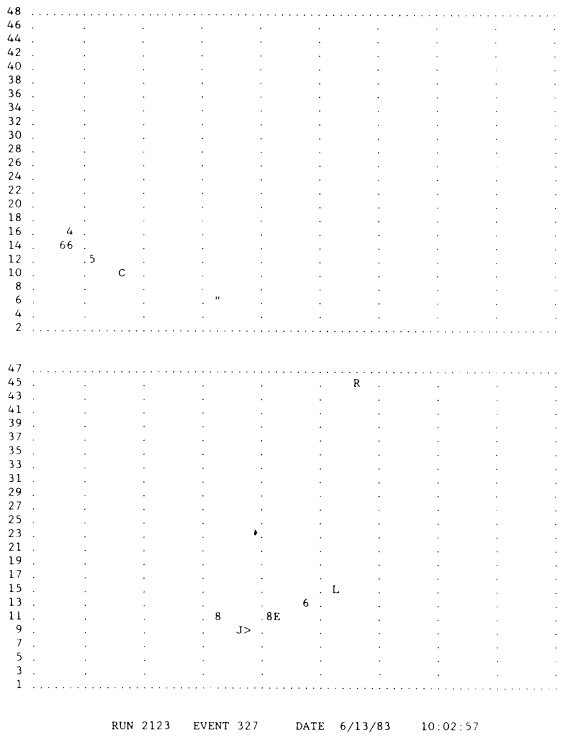

FIG. 8. The second nucleon-decay candidate event. See text for a discussion.

that they result from the products (neutrons, photons, or neutral kaons) of muon interactions in the rock surrounding the detector.

In order to utilize these data to set a limit on the lifetime of the nucleon, and on particular decay modes, it was necessary to determine the acceptance for each decay mode.

This procedure, described in a previous publication,[1] submitted Monte Carlo–simulated nucleon decays to the event-selection criteria outlined above. The events selected were then examined and classified as either clear examples of nucleon decay or as events which were not distinguishable from background processes. The events in Figs. 7 and 8 fall into this second category, and we quote nucleon-decay lifetime (and monopole flux) limits based on zero observed events. The nucleon-decay limits are listed in Table I.

E. The search for monopole catalysis

Our Monte Carlo studies have indicated several general features of the acceptance for monopole catalysis events. Below a velocity of $0.002c$, we assumed that monopoles would not produce sufficient ionization to be detected in the proportional tubes. Thus no monopole track would be measurable, and the monopole could only be detected through its catalysis of nucleon decay. This could appear either as a single, isolated decay, or multiple decays, separated in time. We have also examined the possibility of faster, track-producing monopoles also catalyzing decays, as noted above.

The search for isolated nucleon decays has been detailed above. The signatures for spontaneous decay and catalyzed decay were assumed to be identical, and all of our previous analysis was utilized. It is important to

TABLE I. Detector acceptance and lifetime lower limits (90% confidence level) for various nucleon-decay modes.

	Mode	Acceptance fraction	Lifetime/(branching ratio) (yr)
1	$p \rightarrow e^+ \pi^0$	0.34	1.31×10^{30}
2	$p \rightarrow e^+ \rho^0$	0.31	1.19×10^{30}
3	$p \rightarrow e^+ \omega$	0.38	1.46×10^{30}
4	$p \rightarrow \mu^+ K_S$	0.38	1.46×10^{30}
5	$p \rightarrow \nu K^+$	0.07	0.27×10^{30}
6	$n \rightarrow e^+ \pi^-$	0.32	1.34×10^{30}
7	$n \rightarrow e^+ \rho^-$	0.35	1.46×10^{30}
8	$n \rightarrow \nu K_S$	0.18	0.75×10^{30}
9	$n \rightarrow \pi^+ K^-$	0.27	1.13×10^{30}

note that identification of nucleon decay in Soudan 1 is not predicated on the assumption of momentum balance of the decay products. Thus our previous analysis criteria should not eliminate nucleon decays arising from catalysis.

For multiple decays (without a monopole track), we have found that for moderate cross sections the events would have a very distinctive time structure. Even decays nearly coincident in space are often separated in time, and the hits, grouped in time, are recognizable as nucleon decays. Of course, if the catalysis cross section is too small, the probability of two nucleon decays occurring within the detector becomes small. And if the cross section is too large ($X=1000$), the detector is always triggered by decay products from catalysis in the rock. The topology and time structure of these rock events (though unusual) is not distinctive enough to clearly distinguish them from common electromagnetic showers originating in the rock.

For higher velocity monopoles (which do produce tracks), a small or zero catalysis cross section enhances the probability of detection. This is particularly true for monopoles with a velocity greater than $0.01c$, since any decays would be "on time" (not contain late hits), and the decay products' tracks would lower the average ionization per hit tube. For $X=1$, about 10% of the events would fail the high ionization criteria. Almost no events would pass the cuts for $X=100$. (A few could be caught, "accidentally", by the catalysis search, if the decays produce muons. The decays of the muons could then cause enough late hits for the event to meet the criteria for this search.)

The problem is less extreme for the velocity range from $0.01c$ to $0.002c$, where some of the decays would occur significantly later than the trigger time. These events would meet our multiple decay criteria, though they would fail the velocity fit.

Thus, for monopoles faster than $0.002c$, the acceptance is large and generally flat, except for very large catalysis cross sections. For slower monopoles the acceptance varies strongly with velocity and cross section, but is optimum for moderate cross sections ($X=1$).

We have found no events which meet the selection criteria, and which have a topology at all similar to that expected for events containing multiple nucleon decays, with or without a monopole track.

IV. MONOPOLE-FLUX LIMITS

The results from the Monte Carlo determination of the acceptance, and our null result from the data analysis are presented in the form of (90%-confidence-level) flux limits in Table II and in Fig. 9. We present our limits for noncatalyzing monopoles ($X=0$) and for catalysis cross-section factors of $X=0.01$, 1.0, and 100.0. We have found that for $X=1000$ and above, our acceptance is negligible, and we can set no meaningful flux limit; at high velocities, any tracks are completely swamped by the daughter particles of the nucleon decays, while at low velocities, the detector is always triggered by daughters from the rock before the monopole enters the calorimeter. If $X \ll 0.01$, the catalysis probability is so small that the results are identical to the case $X=0$.

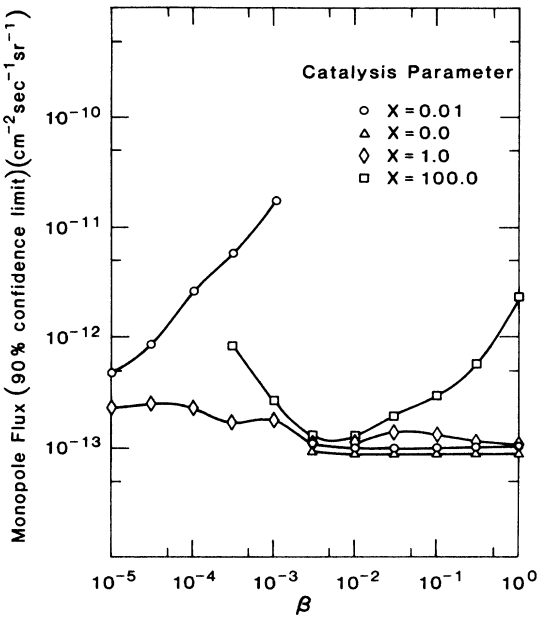

FIG. 9. Flux limits for magnetic monopoles for several values of the nucleon-decay catalysis cross-section parameter X.

For $X=1$, the limit varies between 1.1×10^{-13} and 2.5×10^{-13} monopoles/cm^{2}sec sr over the entire range of velocities considered, the five decades between $v=10^{-5}c$ and c. Since, in our parametrization, the catalysis cross section also varies by a factor of 10^5 over this range, the relative velocity independence of this result is fortuitous. Other values of X (giving different ranges of cross sections), have strongly velocity-dependent limits. This is due in part to the moderate size of the calorimeter (for small cross sections), but also due to the complications introduced by large catalysis cross sections. The influence of catalysis on otherwise straightforward monopole searches was something of a surprise to us, and the preliminary results of this experiment[1] have been

TABLE II. Upper limits (90% confidence level) on the flux of magnetic monopoles. Results are given for several values of the catalysis parameter X (see text) and are in units of 10^{-13}/cm^{2}sec sr.

v/c	$X=0$	$X=0.01$	$X=1$	$X=100$
1.0	0.88	1.03	1.06	23.3
0.3	0.88	1.03	1.15	5.8
0.1	0.88	1.01	1.32	3.0
0.03	0.88	1.0	1.4	2.0
0.01	0.88	1.0	1.1	1.3
3×10^{-3}	0.93	1.1	1.1	1.3
10^{-3}		175	1.8	2.7
3×10^{-4}		58	1.7	8.5
10^{-4}		26	2.3	
3×10^{-5}		8.6	2.5	
10^{-5}		4.8	2.3	

strongly modified for large cross sections. (The previous limit was quoted in the assumed absence of catalysis.) Two arguments exist which suggest that very large cross sections are possible: the reference value used here of 441 μb is somewhat small for a typical strong-interaction cross section which could characterize the process. In addition, the velocity dependence may be stronger than the $1/v$ assumed here. It has been suggested[23,29] that free proton decay catalysis follows a $1/v^2$ law. In this case, our limits extend downward only to velocities of $10^{-2}c$ or $10^{-4}c$ (for X values of 100 or 0.01, respectively) before event confusion and rock-trigger events reduce our acceptance drastically.

Other experiments on monopole detection have, by and large, not considered the possible effects of large catalysis cross sections on their efficiencies. These experiments range from the early work of Ullman[31] to the results from the Baksan underground cosmic-ray detector,[32] with quoted flux limits below 10^{-14}/cm^{2}sec sr. The large water Cherenkov experiments have also set limits on the flux of monopoles if the catalysis process exists. The lowest of these limits is from the Kamiokande detector,[33] at 2.5×10^{-15} cm^{2}sec sr for certain choices of velocity and cross section. Impressive limits are also set by the IMB experiment.[33] While these Cherenkov experiments depend on catalysis for monopole detection, they do not explicitly recognize the associated problem of premature detector triggers caused by catalysis in the surrounding rock.

The only monopole-search experiments that are unaffected by the presence or absence of nucleon-decay catalysis are induction experiments,[8,9] which have set limits on the flux only as low as 6×10^{-12}/cm^{2}sec sr. Major increases in the size of these experiments will be necessary, however, in order to approach monopole-flux limits which can be reached with other techniques,[34] except for very slow monopoles.

ACKNOWLEDGMENTS

The Soudan 1 experiment has been possible only through the efforts and cooperation of a large number of people. We would like to acknowledge the contributions of Tower-Soudan State Park Manager Donald Logan, and his staff, including H. Chiabotti, J. Greenwalt, J. Korich, A. Kosir, A. Mattson, D. Nagel, A. Zavodnik, and C. Carlon, and also H. Bristol, W. Heikinnen, T. Copie, M. Hirsch, H. Hogenkamp, J. Osen, N. Pearson, D. Wicks, G. Blazey, R. Crook, S. Heilig, C. James, X. Li, D. Jankowski, N. Hill, B. Pancake, R. Taylor, R. Laird, Z. Malloi, S. Saroff, and D. Wahl. Thirty tons of taconite concentrate were donated by the Eveleth Taconite Company, for which we are very grateful. This research was supported by the U.S. Department of Energy and by the Graduate School of the University of Minnesota.

---

*Present address: Stanford Linear Accelerator Center, Stanford, California.

[1]J. Bartelt *et al.*, Phys. Rev. Lett. **50**, 651 (1983); **50**, 655 (1983). See also, J. Bartlet, Ph.D. thesis, University of Minnesota, 1984.

[2]M. Marshak *et al.*, Phys. Rev. Lett. **54**, 2079 (1985); J. Bartelt *et al.*, Phys. Rev. D **32**, 1630 (1985); M. Marshak *et al.*, Phys. Rev. Lett. **55**, 1965 (1985).

[3]P. A. M. Dirac, Proc. R. Soc. London **A133**, 60 (1934).

[4]A summary is given by M. J. Longo, Phys. Rev. D **25**, 2399 (1982).

[5]G. 't Hooft, Nucl. Phys. **B79**, 276 (1974).

[6]A. M. Polyakov, Pis'ma Zh. Eksp. Teor. Fiz. **20**, 430 (1974) [JETP Lett. **20**, 194 (1974)].

[7]B. Cabrera, in *Magnetic Monopoles*, proceedings of the Workshop, Racine, Wisconsin, edited by R. A. Carrigan, Jr. and W. P. Trower (Plenum, New York, 1983), p. 175. See also Phys. Rev. Lett. **48**, 1378 (1982).

[8]B. Cabrera, M. Taber, R. Gardner, and J. Bourg, Phys. Rev. Lett. **51**, 1933 (1983).

[9]J. Incandela *et al.*, Phys. Rev. Lett. **53**, 2067 (1984).

[10]D. Gross and M. Perry, Nucl. Phys. **B226**, 29 (1983); R. Sorkin, Phys. Rev. Lett. **51**, 87 (1983).

[11]Ya. B. Zeldovich and M. Yu. Kholopov, Phys. Lett. **79B**, 239 (1978).

[12]J. P. Preskill, Phys. Rev. Lett. **43**, 1365 (1979).

[13]A. Bais and S. Rudaz, Nucl. Phys. **B170**, 507 (1981).

[14]P. Langacker, Phys. Rep. **72**, 185 (1981).

[15]A. D. Linde, Phys. Lett. **108B**, 389 (1982).

[16]A. Albrecht and P. J. Steinhardt, Phys. Rev. Lett. **48**, 1220 (1982).

[17]W. Collins and M. S. Turner, Phys. Rev. D **29**, 2158 (1984).

[18]P. R. Lindblom and P. J. Steinhardt, Phys. Rev. D **31**, 2151 (1985).

[19]M. S. Turner, E. N. Parker, and T. J. Bogdan, Phys. Rev. D **26**, 1296 (1982).

[20]G. Lazarides, Q. Shafi, and T. Walsh, Phys. Lett. **100B**, 21 (1981).

[21]D. M. Ritson, SLAC Report No. 2950, 1982 (unpublished).

[22]S. P. Ahlen, T. M. Liss, and G. Tarle, Phys. Rev. Lett. **51** 940 (1983).

[23]V. A. Rubakov, Pis'ma Zh. Eksp. Teor. Fiz. **33**, 658 (1981) [JETP Lett. **33**, 644 (1981)]; Nucl. Phys. **B203**, 311 (1982).

[24]C. G. Callan, Jr., Phys. Rev. D **26**, 2058 (1982).

[25]T. Fields and D. Jankowski, Nucl. Instrum. Methods **215**, 131 (1983).

[26]W. W. M. Allison and J. H. Cobb, Annu. Rev. Nucl. Part. Sci. **30**, 258 (1980).

[27]X. Q. Li and E. N. May, Soudan Internal Report No. PDK-25, 1981 (unpublished).

[28]The EGS code system, R. Ford and W. Nelson, SLAC internal Report No. 210, 1978 (unpublished).

[29]J. Arafune and M. Fukugita, Phys. Rev. Lett. **50**, 1901 (1983).

[30]The live time for nucleon-decay data is slightly less than the nominal 1.01 yr due to a few days in which the active shield, crucial for nucleon decay, was not operating.

[31]J. D. Ullman, Phys. Rev. Lett. **47**, 289 (1981).

[32]E. N. Alexeyev *et al.*, Lett. Nuovo Cimento **35**, 413 (1982).

[33]T. Kajita *et al.*, J. Phys. Soc. Jpn. **54**, 4065 (1985). For limits from the IMB detector, see S. Errede *et al.*, Phys. Rev. Lett. **51**, 245 (1983).

[34]See, for example, H. Frisch, in *Magnetic Monopoles* (Ref. 7), p. 515.